



Studies of electrochemical properties of TiNi alloy used as an MH electrode. II. Discharge kinetics

C. S. Wang*, Y. Q. Lei and Q. D. Wang

Department of Materials Science and Engineering, Zhejiang University, Hangzhou 310027, PR China

(Received 29 October 1997; in revised form 12 January 1998)

Abstract—The electrochemical polarization and concentration polarization during the discharge of TiNi alloy electrodes are analyzed in terms of a model presented in part I. The ratio of electrochemical polarization to concentration polarization during discharge $(\eta_e/\eta_c)_p$ increases with the number of charge/discharge cycles due to the faster decline in electrocatalytic performance (I_0) than in the apparent diffusion coefficient D_x^A , but the ratio decreases with increasing discharge current density and state of discharge (SOD). However, the ratio of electrochemical polarization to concentration polarization at the end of discharge $(\eta_e/\eta_c)_e$ increases with discharge current density. In contradiction to the generally accepted idea, the discharge capacity is controlled by the rate controlling step at the end of discharge, the discharge capacity has no relationship with the rate controlling step in discharge process. At low discharge current density ($I < I_{dc}$), for which the electrochemical polarization is lower than 0.11 V, the diffusion of hydrogen from the bulk through the oxide film to the surface of electrode is the step controlling of the discharge capacity. However when the discharge current density is higher than I_{ec} , for which the electrochemical polarization is higher than 0.199 V, but lower than the electrochemically limited current density $I_{Le} [= I_0 \exp(0.332\beta F/RT)]$, the discharge capacity is determined by the charge-transfer reaction on the electrode surface. When discharge current density is between I_{dc} and I_{ec} , both electrochemical reaction and hydrogen diffusion limit the discharge capacity. © 1998 Elsevier Science Ltd. All rights reserved

LIST OF SYMBOLS

$C_{\alpha\beta}, C_{\beta\beta}$	The hydrogen concentration of α or β phase equilibrating with P_{eq} at the interface between the α and β phase (mol cm^{-3})	I_{dc}	Maximum discharge current density for concentration polarization controlling (mA g^{-1})
C_{max}	Hydrogen concentration of β phase equilibrating with 1 atm pressure (mol cm^{-3})	I_{ec}	Minimum discharge current density for electrochemical polarization controlling (mA g^{-1})
D_x^A	Appearance hydrogen diffusion coefficient in α phase including hydrogen diffusion through the oxide film at the surface and transfer from the adsorbed sites to adsorbed sites ($\text{cm}^2 \text{s}^{-1}$)	I_{mc}	Discharge current density for mixing controlling (mA g^{-1})
f	Ratio of $\partial Q_d/\partial I_0$ to $\partial Q_d/\partial(D_x^A/r_0^2)$ ($\text{g mA}^{-1} \text{s}^{-1}$)	I_{Ld}	Diffusion limiting current density (mA g^{-1})
$1/k$	Barrier coefficient of phase transformation (mol s g^{-1})	I_{Le}	Electrochemical limiting current density (mA g^{-1})
Q_d, Q_{max}	Discharge capacity and the maximum discharge capacity (mA h g^{-1})	r_0	Average radius of the particle (cm)
I_d	Discharge current density (mA g^{-1})	ρ	Density of TiNi alloy (g cm^{-3})
I_c	Charge/discharge cycling current density (mA g^{-1})	F	Faraday's constant, 96547.6 ($\text{J V}^{-1} \text{mol}^{-1}$) or 26800 mA h
I_0	Exchange current density (mA g^{-1})	η_e	Electrochemical polarization (V)
		η_c	Concentration polarization (V)
		η	Overpotential at the end of discharge (0.332 V)

INTRODUCTION

The use of metal hydrides (MH) as negative electrodes in alkaline rechargeable cells is becoming

*Author to whom correspondence should be addressed.
Fax: 86 571 7951358; E-mail: phycsw@cma.zju.edu.cn

popular, owing to the advantages of the metal hydrides over conventional anode materials in specific energy, cycle life and environmental compatibility.

It is generally accepted that the discharge capacity of a hydride electrode depends both on the amount of absorbed hydrogen in the alloy (determined by P - C - T curves) and discharge kinetics. The latter is determined by the exchange current density and diffusion ability of hydrogen in the alloy [1]. As for the discharge kinetics, increasing both the diffusion coefficient and the exchange current density improves the discharge efficiency, however the discharge efficiency depends more on their controlling steps. Using electrochemical impedance spectroscopy (EIS), Zheng *et al.* [2] showed that the rates of charge and discharge are controlled by the kinetics of the charge transfer reaction on the alloy surface. Yang *et al.* [3] found that for alloys $Ti_{0.35}Zr_{0.65}Ni_xV_{2-x-y}Mn_y$ ($x = 0-0.2$, $y = 0.2-0.4$) with $I_0 = 67-128$ mA/g, at low discharge current density, the charge-transfer reaction is the controlling step of discharge, whereas at high discharge current densities, hydrogen diffusion in the α phase and oxide film is rate-determining, which means that the high-rate dischargeability depends more on the diffusion ability of hydrogen in the alloy and depends less on the electrocatalytic properties of alloys. However the electrode of $M_mNi_{3.6}Mn_{0.4}Al_{0.3}Co_{0.7}$ powder mixed with highly electrocatalytic RuO_2 powder [4] and the electrode of $La_{0.8}Nd_{0.2}Ni_{3.6}Co_{0.2}Si_{0.1}$ containing $MoCo_3$ precipitate-phase [5] both exhibit high high-rate dischargeability. Vidts *et al.* [6] developed equations which describe the mass transfer in the electrolyte and in the solid metal-hydride particles, the ohmic loss in the electrolyte and in the solid phase and a charge-transfer reaction on the surface of the metal-hydride particles. From their model they concluded that the diffusion of atomic hydrogen from the bulk of MH particles to the surface of the particles becomes more limiting when the rate of discharge is increased and when the diameters of the MH particles are increased. So there exist big diversities in the controlling steps both in theory and in experiment results. Therefore fundamental studies on the kinetics of charge/discharge process are required.

Based on the theory developed in part I, we studied the ratio of the electrochemical polarization to the concentration polarization in charge/discharge cycles and during the discharge process. We found that at a certain state of discharge, with increasing discharge current density the hydrogen diffusion from the bulk to the surface of the electrode gradually becomes the limiting step, which is in agreement with many literature reports, but at the end of discharge, the charge-transfer reaction on the electrode surface is the controlling step when discharge current density is high. Also the discharge capacity

is determined by the controlling step at the end of discharge.

The polarization equation of TiNi alloy electrode

As stated in our model of part I, the discharge kinetics depend on both the rate of hydrogen diffusion from the bulk through the oxide film to the surface of the electrode and the rate of the charge-transfer reaction on the electrode surface.

According to equations (7) and (9) in part I and $\eta = \eta_c + \eta_e$:

Concentration polarization:

$$\eta_c = -\frac{RT}{\beta F} \times \ln \left\{ 1 - \frac{I_d r_0^2 \rho}{3FC_{\alpha\beta} D_\alpha} \left(\frac{D_\alpha \rho}{k(C_{\beta\alpha} - C_{\alpha\beta})r_0^2} + 1 \right) \times \left[\left(1 - \frac{Q_d}{Q_{\max}} \right)^{-1/3} - 1 \right] \right\} \quad (1)$$

where Q_d/Q_{\max} is defined as the state of discharge, SOD: $SOD = Q_d/Q_{\max}$.

Electrochemical polarization:

$$\eta_e = \frac{RT}{\beta F} \times \ln \left(\frac{I_d}{I_0} \right) \quad (2)$$

where

$$\frac{C_{\beta\alpha}}{\rho} = 8 \times 10^{-3} \exp \left(-\frac{0.0513N^{1/2}}{I_c^{1/2}} \right),$$

$$\frac{C_{\alpha\beta}}{\rho} = 9.38 \times 10^{-4} \exp \left(-\frac{0.0513N^{1/2}}{I_c^{1/2}} \right) \quad (3)$$

$$\frac{D_\alpha^A}{r_0^2} = 1.87 \times 10^{-4} \exp \left(-\frac{0.01414}{I_c^{1/2}} N^{1/2} \right) \quad (4)$$

$$I_0 = 35 \times \left[\exp \left(-\frac{0.3535}{I_c^{1/2}} N^{1/2} \right) - 0.9 \times \exp \left(-\frac{17.7N^{1/2}}{I_c^{1/2}} \right) \right] \quad (5)$$

$$k = 4.16 \times 10^{-2} \exp \left(\frac{10.25N}{I_c^{1/2}} \right) \quad (6)$$

$$f = \frac{\partial Q_d / \partial I_0}{\partial Q_d / (\partial (D_\alpha^A / r_0^2))} = \frac{D_\alpha^A}{r_0^2 I_0} \left(\frac{1}{I_{Le} / I_d - 1} \right) \quad (7)$$

We regard the process to be controlled by hydrogen diffusion when the value of η_e/η_c is smaller than 0.5, by the electrochemical reaction when the ratio is larger than 1.5 and by both steps when the value is between 0.5 and 1.5.

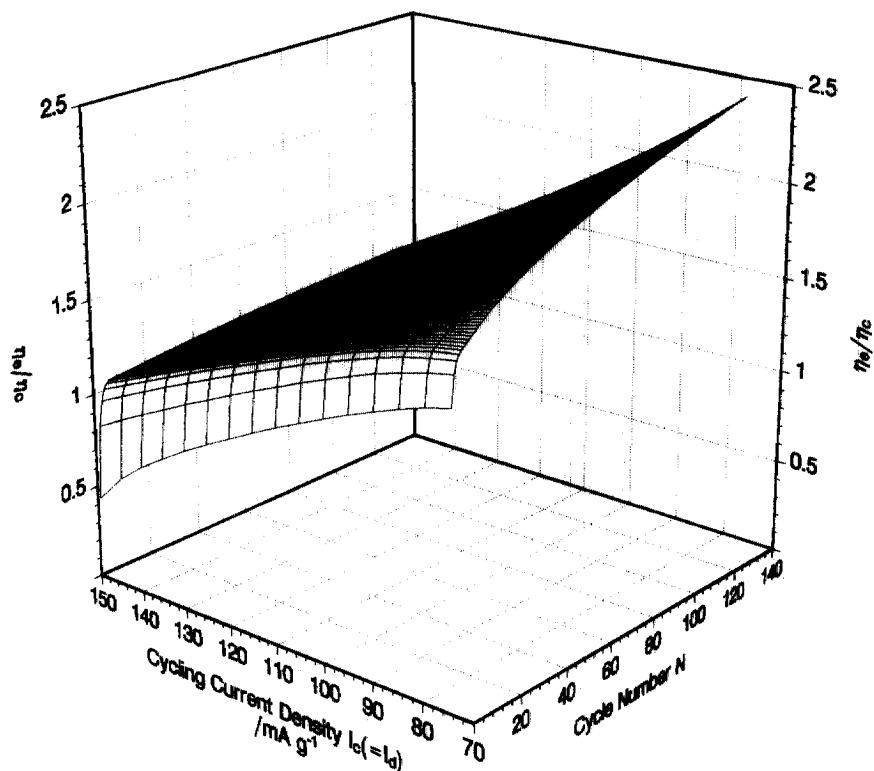


Fig. 1. Plot of (η_e/η_c) vs the cycle number and cycling current density ($I_c = I_d$) for TiNi alloy electrode at 50% SOD.

RESULTS AND DISCUSSION

The ratio of electrochemical polarization to concentration polarization at 50% state of discharge $(\eta_e/\eta_c)_{50\%}$ in the charge/discharge cycle

According to equations (1)–(6), the value of η_e/η_c varies with SOD, discharge current density, cycling current density, cycle number and exchange current density. Figure 1 is the plot of $(\eta_e/\eta_c)_{50\%}$ with the cycle number and the cycling current density at $I_d = I_c$ for the TiNi alloy electrode.

At 50% SOD, $(\eta_e/\eta_c)_{50\%}$ of the TiNi alloy electrode increases with cycle number rapidly during activation due to the quick decrease of the concentration polarization induced by the phase transformation, so the phase transformation is the controlling step during activation. After being fully activated, $(\eta_e/\eta_c)_{50\%}$ increases with the cycle number, which means that oxidation of the TiNi alloy causes a quicker decline in the rate of charge-transfer reaction than that of hydrogen diffusion ability. This can be seen clearly in equations (4) and (5). At low cycle current density the value of $(\eta_e/\eta_c)_{50\%}$ is larger than 1.5, so the charge-transfer reaction on the electrode surface is the limiting step, but at a high cycle current density the value of $(\eta_e/\eta_c)_{50\%}$ is around 1, in the range of mixed control of the charge-transfer reaction and hydrogen diffusion. For the TiNi electrode, the maximum cycling current density during activation is within 150 mA/g with a cut-off potential of 0.6 V vs Hg/HgO at 50%

SOD. After activation the maximum cycling current density can reach 190 mA/g. With further increase of the cycling current density, the SOD will be less than 50%.

The ratio of electrochemical polarization to concentration polarization in discharge process $(\eta_e/\eta_c)_p$ at $I_c = 50$ mA/g, $N = 10$

Figure 2 shows the relationship between η_e/η_c , SOD and discharge current density during discharge. In Fig. 2 the value of $(\eta_e/\eta_c)_p$ decreases with increasing SOD and discharge current density, depending mainly on SOD. For a fully charged TiNi electrode, at a low discharge current density, 80 mA/g, $(\eta_e/\eta_c)_p$ decreases from 24.8 to 0.3 with increasing SOD values from 7 to 76%, i.e. the controlling step changes from the electrochemical reaction to the diffusion of hydrogen. But at a high discharge current density 500 mA/g, $(\eta_e/\eta_c)_p$ decreases only from 10.14 to 0.95 with an increase of SOD from 7 to 25%, i.e. the controlling step changes from the charge-transfer reaction to joint control. Increasing the discharge current density further, the electrochemical reaction controls the discharge process. At 40% SOD, $(\eta_e/\eta_c)_{40\%}$ decreases from 2.82 to 0.69 as discharge current density increases from 80 to 260 mA/g, i.e. the controlling step changes from electrochemical reaction on the TiNi electrode surface to the diffusion of hydrogen in alloy. This is in agreement with the experiment results for $Ti_{0.35}Zr_{0.65}Ni_xV_{2-x-y}Mn_y$

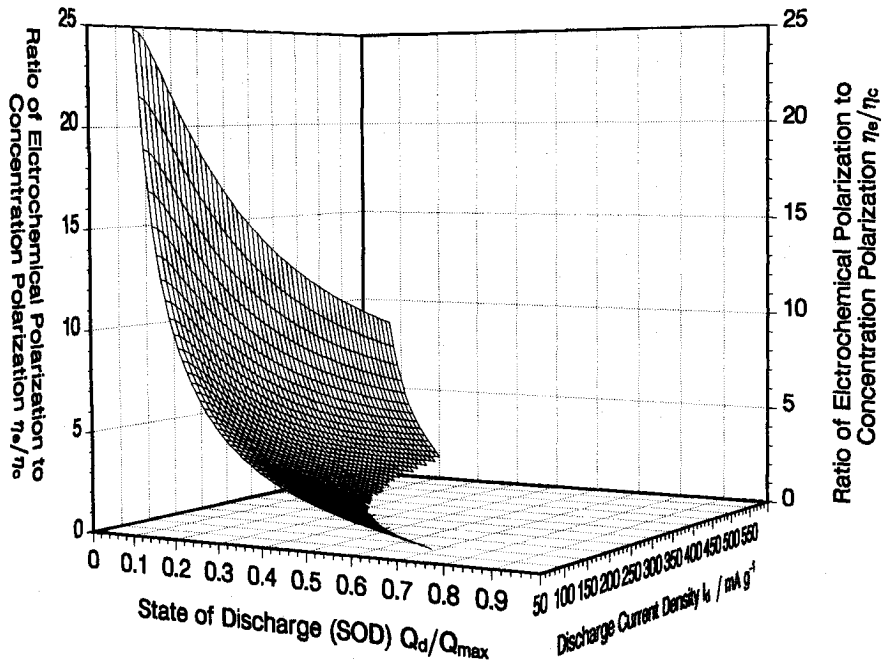


Fig. 2. Relationship between $(\eta_e/\eta_c)_p$, state of discharge (SOD) and discharge current density during discharge.

electrode with 30% SOD reported by Yang *et al.* [3]. The reason why $(\eta_e/\eta_c)_p$ decreases with the increase of SOD is due to the fast decrease of diffusion limiting current density I_{Ld} as SOD increases. From equations (3) and (7) of part I, with $C_s=0$, $I = I_{Ld}$ (diffusion limiting current density), I_{Ld} can be expressed as;

$$I_{Ld} = \frac{3FD_\alpha^\Delta C_{\alpha\beta}}{r_0^2 \rho} \left[\left(\frac{D_\alpha^\Delta \rho}{k(C_{\beta\alpha} - C_{\alpha\beta})r_0^2} + 1 \right) \times \left(1 - \frac{Q_d}{Q_{max}} \right)^{-1/3} - 1 \right]^{-1} \quad (8)$$

In the galvanostatic discharge process with increase of discharge capacity the I_{Ld} decreases toward I_d , results in the overpotential of hydride electrode changing abruptly at the end of discharge. Figure 3 shows the calculated diffusion limiting current density of the TiNi electrode at different SOD using equation (8) and parameter values in Table 2 of part I.

From Fig. 3, the I_{Ld} decreases with the increase of SOD, which is in agreement with the experiment results reported by Yang *et al.* [3]. They believed that the hydrogen diffusion limiting current density can be determined in anodic polarization by linear sweep voltammetry at a scan rate of 1 mV s^{-1} and for $\text{Ti}_{0.25}\text{Zr}_{0.65}\text{Ni}_{1.0}\text{V}_{0.6}\text{Mn}_{0.4}$ electrode the hydrogen diffusion limiting current density increases from 180 to 572 mA g^{-1} when the SOD decrease from ~100% (poorly charge state [3]) to 0 (fully charge state). But the value of hydrogen diffusion limiting current density in fully charge state (SOD = 0) is

lower than that calculated from equation (8), because the scan in positive direction increase the SOD. In Fig. 6 of Ref. [3] for an electrode in the fully charge state, when the overpotential was scanned from 0 to 0.3 V using a scan rate of 1 mV s^{-1} , the anode current density increase from 0 to 550 mA g^{-1} . In this period (300 s), the SOD increases about 33 mA h/g and the capacity of the alloy was 300 mA h/g [7], so the SOD increased by 11% at the end of scanning, which caused the measured I_{Lc} lower than the actual value.

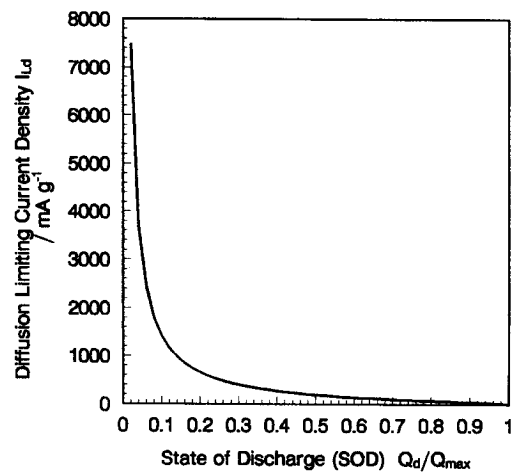


Fig. 3. Relationship between the diffusion limiting current density and SOD for the TiNi electrode using $I_{Ld} = \frac{3FD_\alpha^\Delta C_{\alpha\beta}}{r_0^2 \rho} \left[\left(\frac{D_\alpha^\Delta \rho}{k(C_{\beta\alpha} - C_{\alpha\beta})r_0^2} + 1 \right) \left(1 - \frac{Q_d}{Q_{max}} \right)^{-1/3} - 1 \right]^{-1}$ and parameter values in Table 2 of part I.

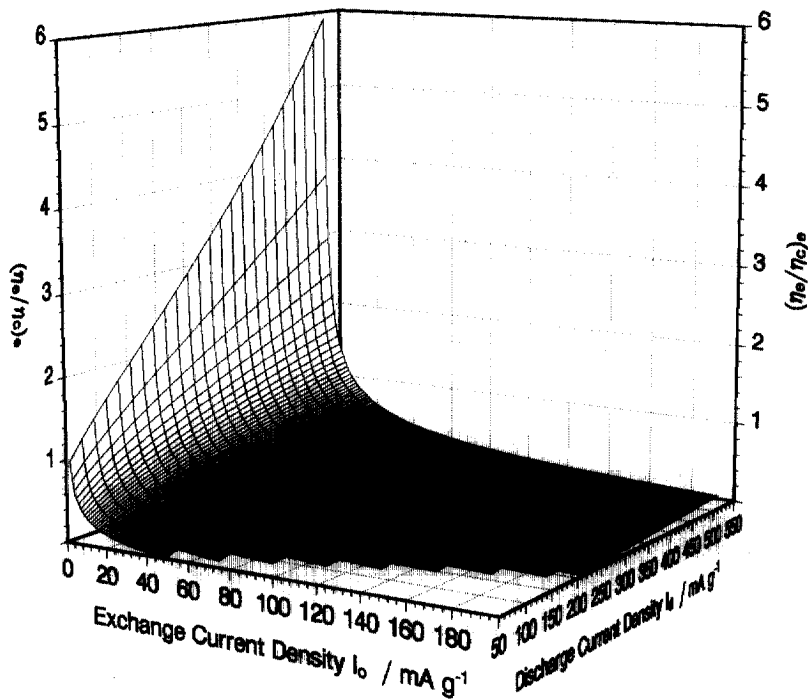


Fig. 4. Relationship between $(\eta_e/\eta_c)_e$, exchange current density and discharge current density at the end of discharge.

The ratio of electrochemical polarization to concentration polarization at the end of discharge for hydride electrode $(\eta_e/\eta_c)_e$

In the anode range, when $\eta \gg RT/F$, $\eta = \eta_e + \eta_c = RT/\beta F \times \ln(I_d/I_0) + \eta_c$. Based on the Nernst equation for metal-hydride electrode, the fully charged potential is -0.932 V vs Hg/HgO [8]. If the cut-off potential set at -0.6 V, the total potential polarization η is 0.332 V at the end of discharge. So $RT/\beta F \times \ln(I_d/I_0) + \eta_c = 0.332$ and $(\eta_e/\eta_c)_e$ can be expressed as

$$\left(\frac{\eta_e}{\eta_c}\right)_e = \frac{RT/\beta F \times \ln(I_d/I_0)}{0.332 - RT/\beta F \times \ln(I_d/I_0)} \quad (9)$$

Figure 4 shows the variation of $(\eta_e/\eta_c)_e$ (at the end of discharge) due to the exchange current density and discharge current density.

The ratio $(\eta_e/\eta_c)_e$ decreases with the increase of exchange current density, but increases with the discharge current density, which is different from the pattern of variation tendency of $(\eta_e/\eta_c)_p$ (during the discharge process). In the discharge the controlling steps change from electrochemical reaction on the surface of electrode to hydrogen diffusion in the α phase and the oxide film with increase of discharge current density at certain SOD as stated in above Section, but at the end of discharge the limiting step changes from hydrogen diffusion to electrochemical reaction with increase of discharge current density, which can also be proved by the discharge curves of the hydride electrode at different discharge current densities. At low discharge current densities

the potential drop is slow initially but becomes drastic at the end of discharge, which indicates that the controlling step changes from the charge-transfer reaction to the hydrogen diffusion during discharge. However when the discharge rate is high, the gentle potential drops reflects the charge-transfer reaction is the limiting step during the whole discharge process, that is the controlling step at the end of discharge changes from the hydrogen diffusion to the charge-transfer reaction when the discharge current density increases. For the TiNi electrode with exchange current density $I_0 = 29.9$ mA/g, at a discharge current density lower than 260 mA/g the diffusion ability of hydrogen controls the discharge of the TiNi electrode ($\eta_e/\eta_c \leq 0.5$), but at higher discharge current densities (between 260 and 1200 mA g⁻¹), the electrochemical reaction and the hydrogen diffusion jointly control the discharge of the TiNi electrode as shown in Fig. 5. In Fig. 10 of part I, it can be seen easily that in the TiNi electrode at a discharge current density lower than 200 mA/g the discharge capacity is controlled by the diffusion ability of hydrogen and at a discharge current density of 500 mA/g, the electrochemical reaction and diffusion ability of hydrogen affect jointly the discharge capacity almost equally. Comparing Figs 2 and 5 with Fig. 10 of part I, we believe the discharge capacity of the TiNi electrode is controlled by the limiting step at the end of discharge, having no relationship with the controlling steps early in the discharge process.

The relationship between the factor limiting the discharge capacity and the step dominating polariz-

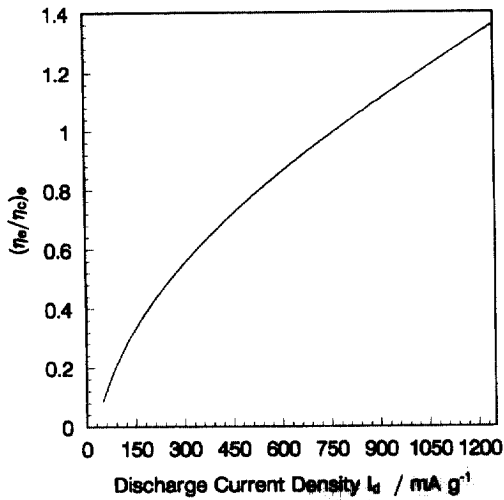


Fig. 5. Relationship between $(\eta_e/\eta_c)_e$ and discharge current density at the end of discharge for the TiNi electrode.

ation at the end of discharge can be obtained by combining equations (7) and (9)

$$f = \frac{\partial Q_d / \partial I_0}{\partial Q_d / (\partial (D_2^A / r_0^2))} = \frac{D_2^A}{r_0^2 I_0} \left(\frac{1}{I_0 \exp((0.332\beta F / [1 + (\eta_e/\eta_c)_e] RT) \eta) - 1} \right) \quad (10)$$

As we expected in equation (10) the value of f increases with $(\eta_e/\eta_c)_e$, so we can predict the factor controlling the discharge capacity from the polarization analysis at the end of discharge. Also the polarization analysis at the end of discharge suits all kinds of hydride electrodes, including AB_3 and AB_2 hydrides.

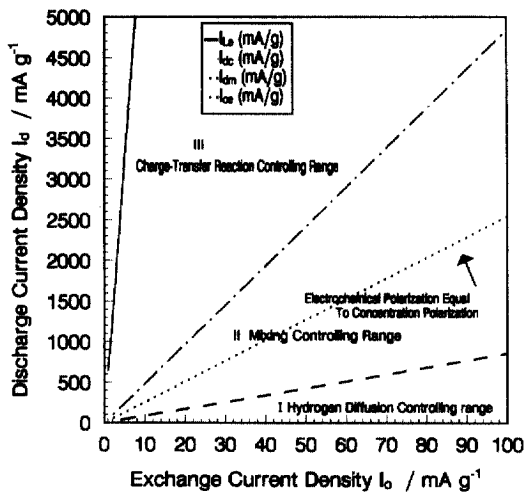


Fig. 6. Plot of controlling step vs discharge current density and exchange current density for hydride electrode.

According to equation (9), the maximum discharge current density for hydrogen diffusion controlling state (at $\eta_e/\eta_c < 0.5$):

$$I_{dc} = I_0 \exp\left(\frac{0.11\beta F}{RT}\right) \quad (11)$$

When the electrochemical polarization is equal to the concentration polarization ($\eta_e/\eta_c = 1$), the process is jointly controlled and the discharge current density can be expressed as:

$$I_{mc} = I_0 \exp\left(\frac{0.166\beta F}{RT}\right) \quad (12)$$

For the electrochemical reaction controlling state (at $\eta_e/\eta_c > 1.5$), the minimum discharge current density is

$$I_{ec} = I_0 \exp\left(\frac{0.199\beta F}{RT}\right) \quad (13)$$

The electrochemical limiting current density I_{Le} is,

$$I_{Le} = I_0 \exp\left(\frac{0.332\beta F}{RT}\right) \quad (14)$$

When the discharge current density is lower than I_{dc} at which the electrochemical polarization is smaller than 0.11 V, the diffusion of hydrogen in the electrode is the determining factor of the discharge capacity. However when the discharge current density is higher than I_{ec} but smaller than the electrochemically limited current density I_{Le} , the electrochemical reaction at the electrode surface is the controlling step. When the discharge current density is between I_{dc} and I_{ec} , at which the electrochemical polarization is close to 0.166 V, the electrochemical reaction and hydrogen diffusion jointly control the discharge capacity. Figure 6 shows the relationship between the controlling step, the discharge current density and the exchange current density of hydride electrodes.

In Fig. 6 the part I region corresponds to control by hydrogen diffusion, part II is the region for control by electrochemical reaction and hydrogen diffusion jointly and part III is the region for control by electrochemical reaction. Generally, for hydride electrodes at low discharge current densities, the hydrogen diffusion is the determining step, but at high discharge current densities the discharge capacity is controlled both by electrochemical reaction and hydrogen diffusion. The above analysis can explain why enhancing the electrocatalytic ability of the hydride electrode such as mixing $M_mNi_{3.6}Mn_{0.4}Al_{0.3}Co_{0.7}$ with highly electrocatalytic RuO_2 powder [4] and $La_{0.8}Nd_{0.2}Ni_{3.0}Co_{0.2}Si_{0.1}$ containing $MoCo_3$ precipitate-phase electrode [5] increases the high-rate dischargeability. Also from

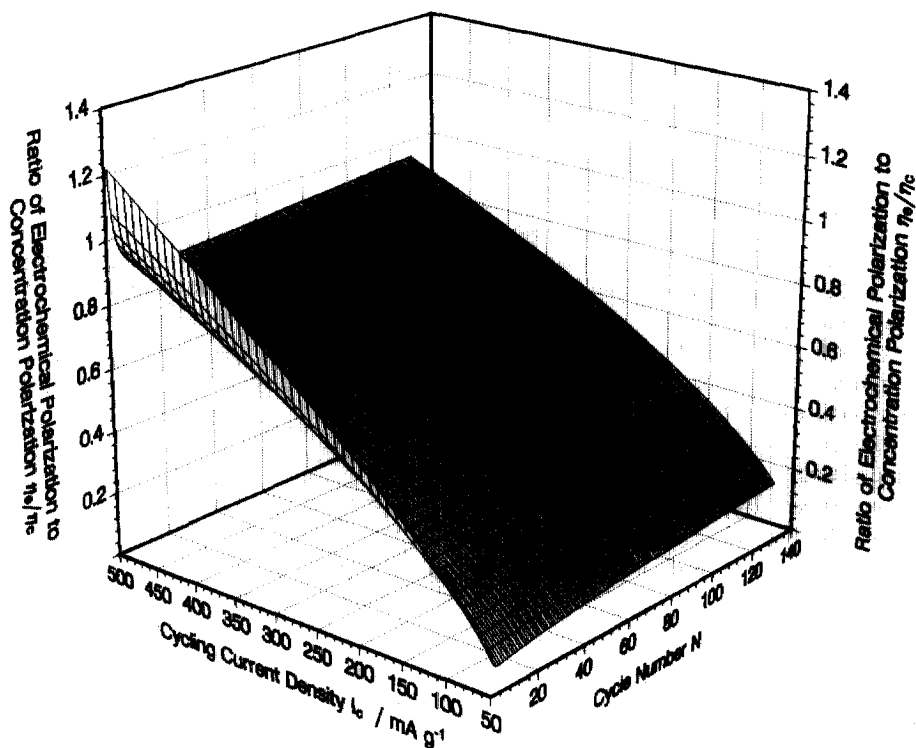


Fig. 7. Relationship between $(\eta_e/\eta_c)_e$ at the end of discharge, cycling current density and cycle number at $I_c = I_d$ for the TiNi electrode.

Fig. 6 we find the hydride electrode with high electrocatalytic capability ($I_0 > 50$ mA/g), the discharge capacity is still controlled by the diffusion ability of hydrogen even at very high discharge current densities (430 mA/g)

The ratio of electrochemical polarization to concentration polarization at the end of discharge $(\eta_e/\eta_c)_e$ in a charge/discharge cycle for the TiNi electrode

Figure 7 shows the relationship between $(\eta_e/\eta_c)_e$ (at the end of discharge), cycling current density and cycle number at $I_c = I_d$ for TiNi electrode.

In contradiction with the results of $(\eta_e/\eta_c)_p$ during charge/discharge cycling, during the activation $(\eta_e/\eta_c)_e$ (at the end of discharge) decreases with cycle number, but after activation is ended $(\eta_e/\eta_c)_e$ increases with cycle number due to the increase of SOD during activation and decrease of SOD as cycling continues. $(\eta_e/\eta_c)_e$ also increases with discharge current density. For the TiNi electrode, at low discharge current densities (< 200 mA g⁻¹), the value of $(\eta_e/\eta_c)_e$ is smaller than 0.5 within 130 cycles, i.e. the diffusion ability of hydrogen in the TiNi alloy is the rate controlling step. When the discharge current density is increased to 500 mA/g, the value of $(\eta_e/\eta_c)_e$ is still smaller than 1.22. It can thus be concluded that during discharge at current densities between 200 and 500 mA/g, the discharge

capacity is controlled jointly by the electrochemical reaction and diffusion of hydrogen.

CONCLUSION

(1) For the TiNi alloy electrodes, when discharge current density is low, the controlling step during discharge changes from charge-transfer reaction on the TiNi alloy electrode surface to hydrogen diffusion in the α phase (including TiO₂ oxide film). When the discharge current density increases, the limiting step during discharge varies from charge-transfer control to the joint control by charge-transfer reaction and hydrogen diffusion and when discharge current density is high, the charge-transfer reaction would control the whole discharge process. During the activation phase, transformation is the controlling step. After activation, when the cycling current density is low, the charge-transfer reaction is the controlling step during discharge, but when the cycling current density is high, the charge-transfer reaction and hydrogen diffusion are jointly the limiting steps of the discharge process.

(2) The discharge capacity of the TiNi electrode is controlled by the determining step at the end of discharge and has no relationship with the controlling step in early discharge process. When the discharge current density lowers to the value $I_{dc} = I_0 \exp(0.11\beta F/RT)$ at which the electrochemical polarization is lower than 0.11 V, the diffusion of

hydrogen in the electrode is the limiting factor. However when the discharge current density is higher than $I_{ec} = I_0 \exp(0.332\beta F/RT)$ and lower than the electrochemically limited current density $I_{Le} = I_0 \exp(0.332\beta F/RT)$, the controlling factor is charge-transfer reaction on TiNi alloy electrode surface and when the discharge current density is between I_{dc} and I_{ec} , at which the electrochemical polarization is near to 0.166 V, the controlling factors are the joint of charge-transfer reaction and hydrogen diffusion. Also the polarization analysis at the end of discharge is suitable for all kinds of hydride electrodes, including AB₃ and AB₂ hydride.

(3) For the TiNi electrode during activation the $(\eta_e/\eta_c)_e$ (at the end of discharge) first decreases with charge/discharge cycle, but after activation the $(\eta_e/\eta_c)_e$ increases with charge/discharge cycle number due to the increase of SOD during activation and then decrease of SOD with charge/discharge cycle.

ACKNOWLEDGEMENTS

The authors acknowledge the financial support from the National Natural Science Foundation of China.

REFERENCES

1. Y. Q. Lei, C. S. Wang, X. G. Yang, H. G. Pan, J. Wu and Q. D. Wang, *J. Alloys Compounds* **231**, 611 (1995).
2. W. Zhang, M. P. Sridhar Kumar and S. Srinivasan, *J. Electrochem. Soc.* **142**, 2935 (1995).
3. H. W. Yang, Y. Y. Wang and C. C. Wan, *J. Electrochem. Soc.* **143**, 429 (1996).
4. C. Iwakura, M. Matsuoka and T. Kohno, *J. Electrochem. Soc.* **141**, 2306 (1994).
5. P. H. L. Notten and P. Hokkeling, *J. Electrochem. Soc.* **138**, 1877 (1991).
6. P. D. Vidts, J. Delgado and R. E. White, *J. Electrochem. Soc.* **142**, 4006 (1995).
7. H. W. Yang, S. N. Jeng, Y. Y. Wang and C. C. Wan, *J. Alloys Compounds* **227**, 69 (1995).
8. C. S. Wang, X. H. Wang, Y. Q. Lei, C. P. Chen and Q. D. Wang, *Int. J. Hydrogen Energy* **22**, 1117 (1997).